Polymer-induced ordering in water-oil-surfactant mixtures

D. Vollmer*
Institute of Physical Chemistry, University of Basel, Klingelbergstrasse 80, CH-4056 Basel, Switzerland

J. Vollmer
Institute of Physics, University of Basel, Klingelbergstrasse 82, CH-4056 Basel, Switzerland

B. Stühn
Institute of Physics, University of Freiburg, Hermann-Herder-Strasse 3, D-7800 Freiburg, Germany

E. Wehrli
Institute of Cell Biology, Eidgenössiche Technische Hochschule Zürich, Schmelzbergstrasse 7, CH-8092 Zürich, Switzerland

H.-F. Eicke
Institute of Physical Chemistry, University of Basel, Klingelbergstrasse 80, CH-4056 Basel, Switzerland
(Received 7 February 1995)

Small angle x-ray scattering (SAXS), freeze-fracture electron microscopy, and differential scanning microcalorimetry are used to investigate the temperature dependent microstructure of water-oil(isooctane)-surfactant(sodium di-2-ethylhexyl sulfosuccinate) mixtures containing variable concentrations of triblock copolymer (polyethyleneoxid-polyisoprene-polyethyleneoxid). Micrographs demonstrate that close to room temperature the microstructure consists of water droplets embedded in an oil matrix. Under increasing copolymer concentration a pronounced interaction peak shows up in SAXS spectra. This indicates a copolymer-induced transition from random towards locally ordered droplet arrangement. Under increasing temperature one crosses a phase boundary. This causes the position of the interaction peak to shift toward smaller Q values, and up to three further, equidistant peaks occur. Equal distances between peak positions implies a lamellar microstructure. It is shown by microcalorimetric measurements that this transition from a microemulsion into a lamellar phase is entropy driven, even when no copolymers are added. At low copolymer concentration the lamellar phase expels an excess oil phase. However, for sufficiently high copolymer concentration the system remains single phase. Elaborating on this point, we demonstrate that addition of a lipophilic polymer forms a method of stabilizing lamellar phases. Furthermore, the increasing number of peaks in the scattering spectra indicates that the order in the lamellar structure increases significantly by addition of copolymer.

PACS number(s): 61.30.−v, 82.70.Kj, 61.10.−i, 64.70.Ja

I. INTRODUCTION

Lately the study of order-disorder transitions in weak mesophases has attracted much attention. Colloidal particle and block copolymer systems which show several ordered phases, are frequently studied in this context [1–6]. In particular, the ordering of spherical and lamellar structures has been investigated intensively. Similar to these systems water-oil-surfactant mixtures show temperature and composition dependent transitions between more or less structured phases [7–11]. For microemulsions containing a high volume fraction of droplets, small angle neutron scattering [12] and microscopic [13] investigations indicate the formation of structures with a close packing of droplets in a disordered cubic arrangement. Transitions towards lamellar structures can easily be induced [48]. Lamellar structures attracted particular attention, because they allow the investigation of interactions between fluid membranes and of characteristic surface properties [14–17]. Typically surface tension can be neglected in these mixtures. This permits a direct investigation of stabilizing forces of lamellar phases. Besides Van der Waals, hydration and electrostatic forces, thermally induced undulation interactions stabilize the structures [17–19]. Of all these structures only electrostatically stabilized lamellae show a large correlation length at interlamellar distances of tens of nanometer [15,20,21].

In this paper we discuss the influence of triblock copolymers on the formation of ordered phases in water-oil-surfactant mixtures. At room temperature the water and the oil domains form good solvents for the polyethyleneoxid and polyisoprene parts of the triblock copolymer, respectively, as the components of this copolymer form a hydrophilic(PEO)-hydrophobic(PI)-hydrophilic(PEO) sequence [22,23]. It has been shown that the addition of the copolymer stabilizes the droplet phase

*Present address: Institute of Physical Chemistry, University of Mainz, Welder-Weg 11, D-55099 Mainz, Germany.

[22–25]. At sufficiently high copolymer concentration locally ordered [27] viscoelastic networks [28] are formed. In the present article previous results on local ordering of copolymer coated droplets [27] are supported by small angle x-ray scattering (SAXS) measurements, showing a pronounced small-angle peak. This finding is interesting as the droplet volume fraction is far below close packing. Under increasing temperature a microemulsion to lamellar transition is observed for the pure water-oil-surfactant mixture. This structural transition is accompanied by macroscopic phase separation, leading to an excess oil phase. Likewise the copolymer containing microemulsion performs this transition into a lamellar phase. However, we find that the addition of the copolymer stabilizes the lamellar phase, so that at least on the experimental time scale of the measurements presented in this paper, no phase separation arises at sufficiently high copolymer concentration. This is fortuitous as it allows us to determine the latent heat of the phase transition between a droplet and a lamellar phase of equal composition.

When increasing copolymer concentrations SAXS spectra for lamellar phases show up to four well separated peaks. The perpendicular correlation length increases significantly, even for interlamellar distances of tens of nanometers. By replacing copolymers with lipophilic homopolymers we demonstrate that ordering is caused by the entropic forces of the polymers, which act as spacers in the oil layer. This implies that the addition of polymers forms an efficient method to stabilize fluid membrane systems with large interlamellar spacings.

This paper is organized as follows: Sec. II deals with experimental details, including relevant steps needed to be considered for freeze-fracture replication transmission electron microscopic studies, experimental details of SAXS, and microcalorimetric measurements. Section III is devoted to a description of the results. First the relevant part of the phase diagram is discussed. By electron microscopy we show that close to room temperature the microstructure of the sample conforms to droplets. Under increasing temperature the sample undergoes an entropy driven structural transition into a liquid crystalline phase. The microstructures of the low and of the high-temperature phases are examined in Sec. III C and III D. In Sec. IV a qualitative discussion of the origin of polymer induced ordering of the water-oil-surfactant mixtures is given, and the main results are summarized.

II. EXPERIMENT

A. Materials

The microemulsion is prepared from deionized, bidistilled water, from the highest grade commercially available isooctane (2,2,4 trimethylpentane), and from AOT (sodium di-2-ethylhexyl sulfosuccinate). All components are used without further purification. Isooctane (purity $>99.5\,\%$) and AOT (purity $>99\,\%$) are obtained from Fluka, Switzerland. Microemulsion composition is given for all samples by the molar ratio of water to surfactant $w_0=[H_2O]/[AOT]=61.8$ and the volume fraction of water-plus-surfactant $\phi_d=0.27$. The droplet phase of the microemulsion consists of surfactant coated water droplets. The radius of the water core R_w can be calculated by a semiempirical equation [29]

$$R_w \approx (1.4w_0+2.3)\ \text{Å} \approx 9\ \text{nm} . \quad (1)$$

The triblock copolymer is obtained from Gauthier, Canada, where it is prepared by anionic polymerization. It consists of two PEO end blocks with number average molecular weight $M_n^{\text{PEO}}=10\,400\ \text{g mol}^{-1}$ each and a PI middle block with $M_n^{\text{PI}}=49\,000\ \text{g mol}^{-1}$. Polydispersity of the copolymer is given by $M_w^{\text{cop}}/M_n^{\text{cop}}\approx 1.15$. For the densities of PEO and PI we use $\rho_{\text{PEO}}=1.13$ g/ml and $\rho_{\text{PI}}=0.91$ g/ml. Assuming excluded volume interaction of the copolymer coils, each in a good solvent, the end-to-end distance R_{E-E} has been estimated to be $R_{E-E}^{\text{PEO}}\approx 15$ nm for the PEO end groups and $R_{E-E}^{\text{PI}}\approx 28$ nm for the PI middle part [30]. It should be noted that PEO becomes increasingly hydrophobic at high temperatures. To shed light on the mechanism of ordering in the lamellar phase hydrophobic homopolymer PI with number average molecular weight of $M_n^{\text{PI}_{\text{homo}}}=48\,000\ \text{g mol}^{-1}$ is used.

Copolymer mediated microemulsions are prepared by adding appropriate amounts of copolymer to the microemulsion. Depending on copolymer concentration the dispersion is stirred for two up to five days with a magnetic stirrer. Stirring temperatures were chosen as low as possible, as PI easily forms chemical cross links at high temperatures. The viscosity of the solution increases under dissolution of triblock copolymer, while it decreases significantly under increasing temperature [28]. To prepare samples containing high copolymer concentrations, temperatures of at most 313 K were used for mixing during the last two to three days of stirring. The volume fraction of copolymer (ϕ_{cop}) and the corresponding average number of copolymers per droplet R are listed in Table I.

B. Freeze-fracture replication transmission electron microscopy (FFEM)

A 400 mesh copper TEM grid is immersed into a thermostated copolymer mediated water-in-oil microemulsion and then positioned between two copper plates of about 0.1 mm thickness. Thereby the liquid specimen is squeezed between the plates (sandwich method [13,31]). The sandwiches are held together by stainless steel tweezers and quenched by spraying a mixture of 2-methylbutane and propane (90±5 K) at 8 bar onto both sides of the sandwich (propane jet method [32]). After

TABLE I. Volume fraction of triblock-copolymer ϕ_{cop}. In the droplet phase ϕ_{cop} corresponds to R copolymers per droplet on the average. For the calculation of R it is assumed that the number of droplets remains constant after the addition of the copolymer.

$100\phi_{\text{cop}}$	0	1.2	2.9	4.2	6.9	9.7	11.1
R	0	2	4	7	10	15	20

quenching, the sandwich is transferred into liquid nitrogen and brought into a brass block (Balzer). It is mounted in a Balzer freeze-etch device (BAF301) at 123±2 K. The pressure is reduced to 5×10^{-7} m bar. After evacuation the sandwich is fractured by unclasping the brass block. To enhance contrast of the surface topography, the sample is warmed up to 153±2 K and edged for ten minutes. At this temperature oil evaporates more than 100 times faster than water [33]. Thereafter the sample is cooled again at 123±2 K and its surface is shadowed with a 20 Å layer of W-Ta under an angle of 45°. In order to provide sufficient mechanical stability of the W-Ta film, carbon is sputtered under 90°. Finally the specimens are warmed up to room temperature and brought to atmospheric pressure. The replica adhering to the TEM grid is washed in chloroform, dried in the air, and examined with a Philips EM301 microscope.

C. Small angle x-ray measurements (SAXS)

The SAXS experiments are carried out in a Kratky compact camera (Paar, Graz, Austria). The x-ray beam from a Cu anode is filtered with a Ni foil and reflected from a graphite crystal to yield a monochromatic Cu K_α radiation with a wavelength $\lambda=0.154$ nm. The scattered intensity is detected with a scintillation counter and a detector slit of 200 μm in a distance of 260 mm from the sample. The accessible range of scattering angles of $0.15°\leq 2\theta\leq 4.2°$ covers a range of scattering vectors $Q=(4\pi/\lambda)\sin\theta$ between 0.1 and 3 nm^{-1}. The Kratky camera has a resolution in ΔQ of 0.056 nm^{-1}. The samples are contained in sealed Mark capillaries with a wall thickness of 1 mm. They are placed in an oven allowing temperature control with a stability better than 0.5 degrees. The background scattering due to the glass capillary is determined separately and subtracted from the data. It amounts to only a few percent of the scattered intensity. Further data treatment includes desmearing of the data to account for the slit geometry of the primary beam profile using known procedures [34]. The result is the cross section per volume in units of the Thomson cross section $\sigma_{Th}=7.910^{-26}\,cm^2$. The scattering profile is determined by the high electron density of the AOT-head groups. $\rho_{AOT}=850$ e/nm^3 compared to the electron densities of water, isooctane, PEO, and PI given by $\rho_{H_2O}=333$ e/nm^3, $\rho_{iso}=253$ e/nm^3, $\rho_{PEO}=379$ e/nm^3, and $\rho_{PI}=316$ e/nm^3, respectively. The AOT tails essentially have the same electron density as the oil and thus do not contribute to the scattering pattern significantly.

D. Differential scanning microcalorimetry (DSC)

The difference in the specific heat of a copolymer mediated microemulsion with respect to a reference solution is measured as function of temperature with a MicroCal MC-2 differential scanning microcalorimeter [35]. It consists of twin coin shaped, fixed in place cells of 1.22 ml each, mounted in an adiabatic chamber. One of the cells is filled with the copolymer mediated microemulsion. The second cell is filled with a mixture of water and isooctane having approximately the same specific heat. A thermoelectric device measures the temperature difference ΔT between both cells. Any nonzero ΔT signal activates a cell feedback, network, driving ΔT back to zero. When as a result of temperature scanning endothermic (exothermic) reactions occur in the sample cell more (less) power feedback is momentarily required to null ΔT. Up to a linear baseline, $C_p^{base}(T)$, this signal is proportional to the specific heat $C_p^{rel}(T)$. The remainder $\Delta C_p(T)\equiv C_p^{rel}(T)-C_p^{base}(T)$ yields the difference of the specific heat of the copolymer mediated microemulsion and the reference solution. Accuracies of about 200 $\mu J\,K^{-1}\,ml^{-1}$ for $\Delta C_p(T)$ are achieved.

III. RESULTS

A. Phase behavior

Figure 1 shows a phase diagram [25] of a copolymer mediated microemulsion as a function of temperature T and average number of copolymers per droplet R. Depending on temperature and composition the one-phase microemulsion L_2 consists of isolated droplets, clustered droplets or bicontinuous structures [36]. Still, isolated droplets may be left in the latter two phases. The temperature interval where a single phase microemulsion is favored increases with copolymer concentration. Furthermore, the viscosity of the sample increases with copo-

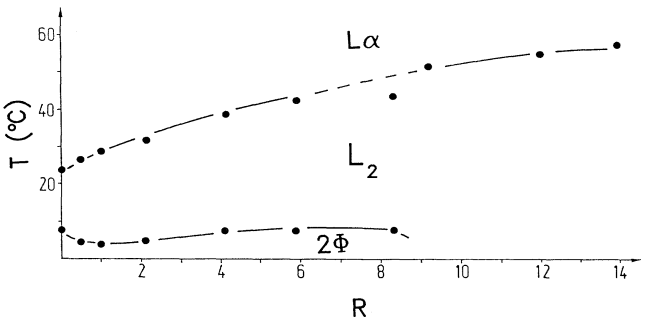

FIG. 1. Phase diagram of a copolymer mediated microemulsion as a function of temperature T and the average number of triblock copolymer (PEO-PI-PEO) per droplet R. For all copolymer concentrations the composition of the microemulsion is given by $w_0=61.8$ and $\phi_d=0.27$. Addition of copolymer leads to a broadening of the temperature region of the one-phase microemulsion phase L_2. For lower temperatures macroscopic phase separation occurs (2ϕ). Passing the upper phase boundary of the L_2 phase gives rise to a structural transition of the copolymer mediated microemulsion into a liquid crystalline phase L_α. Due to the Gibbs–van der Waals principle [26] a two-phase region has to exist along the phase boundary (cf. Fig. 5). For low R values the L_α phase coexists with an excess oil phase (not indicated in the phase diagram). For $R\gtrsim 5$ no sign of macroscopic phase separation could be detected during several days by visual inspection of the L_α phase at 333 K. However, after tempering the samples for more than a week, the transparent solutions became turbid, slightly yellow, due to temperature enhanced chemical cross linking of PI blocks. This reaction goes along with phase separation in most of the cases. (This figure is reproduced from Ref. [25].)

lymer concentration, leading to viscoelastic network formation at sufficiently high concentration [28]. At a fixed temperature this implies a substantial growth of relaxation times. In contrast, the viscosity decreases strongly under increasing temperature [28]. This is probably due to the temperature dependent interaction of PEO with water and oil: PEO becomes increasingly hydrophobic under increasing temperature.

Passing the upper phase boundary leads to a structural transition of the copolymer mediated microemulsion into a liquid crystalline phase L_α. For samples containing low copolymer concentrations ($R \lesssim 4$) the L_α phase coexists with an oil rich phase, whereas for samples containing high concentrations the solution remains single phase for hours up to days. It is not meaningful for the present sample to ask for phase separation on even longer time scales as irreversible network formation of the polymers (PI) becomes increasingly important at these temperatures and time scales.

From the phase diagram one observes that the addition of the copolymer stabilizes the microemulsion phase. Microemulsion phases are only formed by systems with low bending rigidity κ of the surfactant layer, i.e., when κ is of order $k_B T$. For higher bending rigidity ordered phases are formed [8]. This indicates that κ must not change significantly under addition of the copolymer to the sample. This is in agreement with recent studies on homopolymers adsorbing on surfactant bilayers [38].

B. Characterization of the low-temperature phase of FFEM

A priori it is not clear from the phase diagram whether a droplet structure still exists after the addition of the copolymer to the microemulsion. This becomes clear from Fig. 2, showing a FFEM micrograph of a copolymer mediated microemulsion ($R=8, \phi_{cop} \approx 0.05$) at $T=298$ K. The figure demonstrates that the droplet structure is preserved [27]. Similar micrographs are obtained at other compositions: droplets are homogeneously distributed, showing a slight tendency towards a preferred droplet-droplet distance. The average radius of the droplets can be measured directly from the micrograph, yielding 11 ± 3 nm. The error in droplet size is mainly due to a slight polydispersity, a restricted visibility of droplets that are partially buried after the fracture and to difficulties to distinguish droplets from their surroundings. The radius for the droplet size is close to the radius of a pure microemulsion, obtained by geometric considerations $R_d \approx (1.4 w_0 + 2.3)$ Å $+ 10.5$ Å ≈ 10 nm [29], where the tail length of an AOT molecule is taken to be 10.5 Å. In fact, the slight copolymer concentration dependent increase of droplet size is expected as the hydrophilic parts of the copolymer that stick in the water core of the droplets, lead to an effective increase of the water contents.

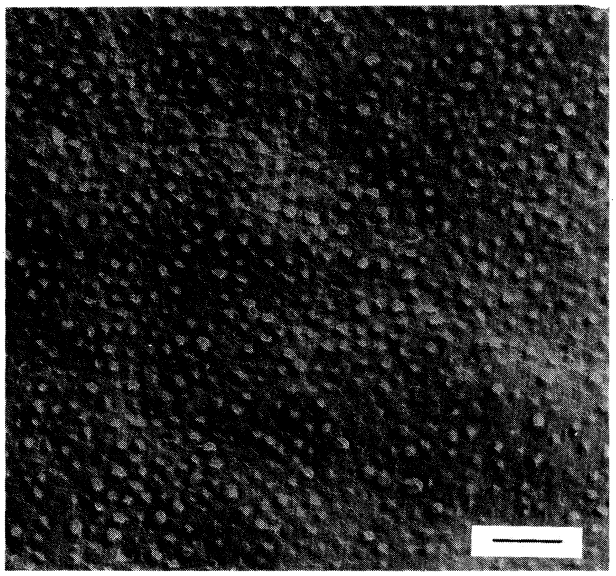

FIG. 2. Freeze-fracture electron micrograph of a copolymer mediated water-in-oil microemulsion at 294 ± 0.5 K in the one-phase region. Water droplets are embedded in an oil matrix. The composition of the copolymer mediated microemulsion is given by: $R=8$, $w_0=61.8$, $\phi_d=0.27$. The length of the bar corresponds to 200 nm.

C. The structural transition of a microemulsion into a liquid crystalline phase

In this subsection we investigate the temperature region close to the upper phase boundary in more detail. SAXS intensity spectra are displayed in Fig. 3 at temperatures 298 K $\leq T \leq 343$ K. Copolymer concentrations are given by $\phi_{cop}=0.069$ [Fig. 3(top)] and $\phi_{cop}=0.11$ [Fig. 3(bottom)], respectively. For $T \lesssim 318$ K the scattering spectra are characterized by a pronounced peak at $Q_1 = Q_d \approx (0.225 \pm 0.005)$ nm^{-1}. For $T \gtrsim 325$ K the position of the first peak shifts towards lower Q values and a second peak occurs. At high copolymer concentration [Fig. 3(bottom)] up to four maxima can be discerned at these temperatures.

The temperature dependent values of the position of the first maximum Q_1 are given in Fig. 4 for $\phi_{cop}=0.069$ (left axis, crosses). $Q_1(T)$ decreases significantly between 318 K and 328 K. For lower and higher temperatures it remains constant within the error margin. Superimposed on the data for $Q(T)$ are the temperature dependent values for the specific heat (triangles, stars; right axis). The thermogram is characterized by a single peak. The position and width of the peak in $\Delta C_p(T)$ agrees with the temperature interval where the value of the scattering vector belonging to the first maximum changes. Comparison with the phase diagram (Fig. 1) demonstrates that the peak as well as the shift in $Q_1(T)$ is due to the transition of the microemulsion phase into the liquid crystalline phase. The size of the two-phase region, separating the microemulsion and the liquid crystalline phase is given by the width of the peak in $\Delta C_p(T)$.

At sufficiently high copolymer concentration data of repeated measurements *without* changing sample material reproduce well. The triangles (first scan) and squares (second scan) in Fig. 4 correspond to values for $\Delta C_p(T)$ of two successive temperature scans without changing sample material. The spectra coincide within the error margin, showing that no indication of phase separation occurs after tempering the sample in the liquid crystalline

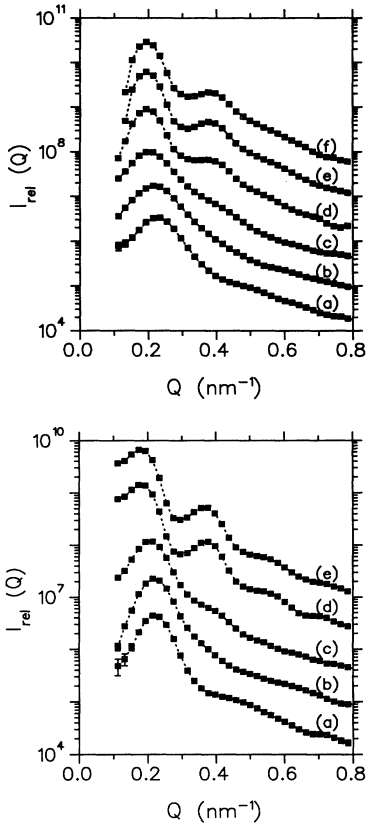

FIG. 3. SAXS spectra showing the temperature evolution of a copolymer mediated microemulsion with composition: $\phi_{cop}=0.069$ or $R=10$ in Fig. 3(top) and $\phi_{cop}=0.11$ or $R=20$ in [Fig. 3(bottom)], respectively. At room temperature the microstructure conforms to droplets. A liquid crystalline phase emerges at $T\gtrsim 329$ K. Temperatures on top: (a) 298 K, (b) 318 K, (c) 325 K, (d) 329 K, (e) 333 K, and (f) 343 K. Temperatures on bottom: (a) 298 K, (b) 318 K, (c) 325 K, (d) 333 K, and (e) 343 K.

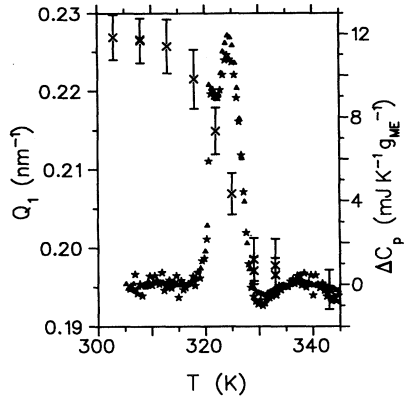

FIG. 4. Compilation of the values of the specific heat C_p and of scattering vectors Q_1 belonging to the maximum of the first peak of the SAXS spectra. The composition of the samples is given by: $\phi_{cop}=0.069$, $w_0=61.8$, $\phi_d=0.27$. Left axis: temperature evolution of the scattering vector Q_1 belonging to the first maximum in $I(Q)$ [cf. Fig. 3(top)]. Q_1 decreases significantly between 318 K and 328 K. Right axis: temperature dependence of the specific heat $\Delta C_p(T)$, per g solution, obtained after subtraction of a baseline and a step. The triangles (first scan) and stars (second scan) correspond to two successive up scans.

phase for 2 h. For low copolymer concentration ($\phi_{cop}\approx 0.02$) the spectra of repeated measurements without changing sample material do not coincide. For those samples the structural transition gives rise to phase separation. Phase separation occurs faster when copolymer concentration is reduced furthermore. This is in agreement with visual inspection of the solutions. For $\phi_{cop}\gtrsim 0.03$ no sign of macroscopic phase separation has been detected when tempering the sample at 333 K up to a week. Due to the decrease of the viscosity at high temperatures, and the well defined peaks in the spectra of specific heat measurements, we believe that equilibration times are well below several hours for the high temperatures where the liquid crystalline phase is formed.

The area under the peak yields a measure for the difference of the enthalpy ΔH between the microemulsion and the liquid crystalline phase. Decreasing copolymer concentration still increases ΔH, indicating that the transition from a microemulsion into a liquid crystalline phase leads to an enthalpy gain. As $\Delta S\approx\Delta H/T$, this strongly suggests that the transition is entropy driven, even when no copolymers are added (cf. Fig. 5).

D. Local order in the low-temperature phase

Figure 6 shows a more detailed SAXS spectrum of a sample with a high copolymer concentration ($\phi_{cop}=0.11, R=20$) at $T=298$ K. Besides the peak at $Q_1\approx 0.225$ nm^{-1} there is a second broad peak at $Q_2\approx 0.45$ nm^{-1}. In order to characterize the structure more quantitatively we fitted the intensity spectra $I(Q)$ by using the relation

$$I(Q)\propto P(Q)S(Q)\ , \tag{2}$$

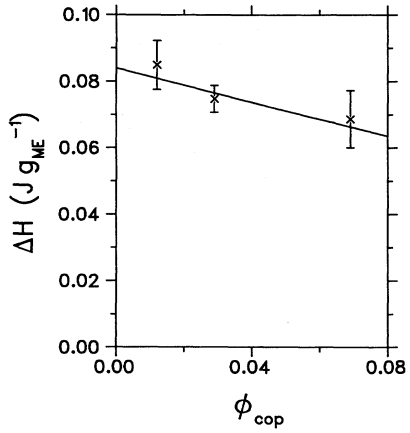

FIG. 5. Values for the enthalpies ΔH per g solution obtained for the transition of a microemulsion of composition $\phi_d=0.27$, $w_0=61.8$ into a liquid crystalline phase for three copolymer concentrations. The solid line yields a linear least square fit and is intended to guide the eye. The errors in data points are mainly due to uncertainties in determining the baseline of DCS spectra.

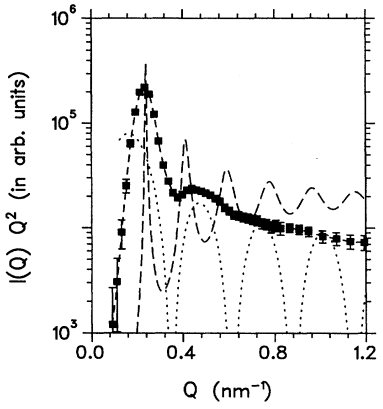

FIG. 6. Small angle x-ray scattering intensities (squares) of a polymer mediated microemulsion at $T=298$ K. The solid line is intended to guide the eye. The structure of the spectra can be explained in terms of a form factor representing the droplet structure of the sample (dotted line), and a structure factor accounting for local ordering of droplets (dashed line), and a linear background (not shown). The broadening of the experimental spectrum with respect to form and structure factor is mainly due to the finite resolution of the Kratky camera. To accentuate peaks in the spectrum the measured intensity and the form factor are multiplied by Q^2.

where $P(Q)$ is the form factor of the droplets and $S(Q)$ the structure factor. On a logarithmic scale this implies $\log[I(Q)Q^2]$ is given by the sum of a constant, of $\log P(Q)$ and of $\log[S(Q)Q^2]$.

The particle form factor represents the scattered intensity from a single isolated sphere with centrosymmetric electron density profile $\rho(r)$,

$$P(Q)=\left[\int_V \rho(r)e^{i\mathbf{Q}\cdot\mathbf{r}}d^3\mathbf{r}\right]^2 . \tag{3}$$

The integral extends over the scattering volume V. For microemulsion droplets the electron density profile is determined by the AOT-head groups, possessing a head group diameter of about 0.18 nm [10,39,40]. This contribution to the scattering intensity is given by the dotted line in Fig. 6.

The structure factor (dashed line in Fig. 6) accounts for contributions to the scattering intensity due to (local) ordering of the droplets. For monodisperse particles Zernike and Prins [41] derived the following relation between $S(Q)$ and the radial distribution function $g(r)$ describing the arrangement of particles

$$S(Q)=1+4\pi n\int_0^\infty [g(r)-1]\frac{\sin Qr}{Qr}r^2dr , \tag{4}$$

where n is the particle number density of droplets. For high particle densities $g(r)$ can be approximated by the Percus-Yevick model [42–44]. As indicated in Fig. 2, copolymer containing microemulsions show a tendency towards a preferred droplet-droplet distance, which becomes more pronounced under increasing copolymer concentration [27]. For spherical hard core particles surrounded by a coat of other molecules Fournet generalized Eq. (3), leading to an increased minimum distance between centers of hard spheres from $2R_d$ to $2R_{\rm eff}$ [45]. Using this theory we fitted our spectra using two radii, one related to the size of the water core being bordered by AOT head groups, and a second related to the radius of an effective hard-core region $R_{\rm eff}$. For the radius of the water core we obtain $R_w=(11.2\pm0.6)$ nm, and for the effective hard-core interaction radius $R_{\rm eff}=(16.5\pm1)$ nm. As the volume fraction of the water core is fixed by composition ($\phi_c=0.22$) we obtain for the volume fraction of the surfactant coated water droplets $\phi_{\rm eff}=\phi_c[R_{\rm eff}/R_w]^3\approx0.66\pm0.08$, which is only slightly below the volume fraction of close packing. The latter value is expected from a more naive interpretation of the SAXS spectra: assuming locally a closed packed structure, the first-order diffraction condition is given in terms of the hard-core radius $R_{\rm HC}$ of the particles [12,46]

$$Q_1=\frac{\pi\sqrt{6}}{2R_{\rm HC}} \implies R_{\rm HC}\approx 17 \text{ nm} , \tag{5}$$

showing that the effective interaction radius $R_{\rm eff}$ coincides within the error margin to the hard-core radius. Moreover, for the data to be consistent these radii have to coincide with half the droplet-droplet distance $\bar{d}$ determined from geometrical parameters (again close packing is assumed),

$$\begin{aligned}\tfrac{1}{2}\bar{d}&=2^{-3/2}\left[\frac{4}{n}\right]^{1/3}\\&=2^{-3/2}\left[\frac{16\pi R_w^3}{3(\phi_w+\phi_{\rm PEO})}\right]^{1/3}=16 \text{ nm} ,\end{aligned} \tag{6}$$

where we used

$$R_w=\left[1.4w_0\frac{\phi_w+\phi_{\rm PEO}}{\phi_w}+2.3\right]\text{ Å}\approx 10.3 \text{ nm} \tag{7}$$

in generalization to Eq. (1). The radii determined from the composition underestimate those determined from experimental data by a few percent. However, this deviation is not significant, because the surface area per surfactant molecule enters both constants in (1), and it is well known that this quantity varies with droplet size and temperature [40].

The consistency of the data indicates that the first and partially also the second peak occur from interparticle interference of radiation from polymer coated microemulsion droplets. Including corrections for droplet polydispersity and diffuse sphere boundaries would desmeare the minima between the peaks, for both, the contributions of the form factor and the structure factor to the scattering spectrum. By doing this we do not expect to obtain significantly more information on the structure of the system, as the width of the measured peaks is mainly determined by the Q resolution of the Kratky camera of 0.056 nm^{-1}.

E. Structure of the high-temperature phase

To obtain more detailed information on the microstructure of the high-temperature L_α phase we investigate the values of the scattering vectors belonging to the

maxima in the scattering intensity. As the scattering spectrum belonging to the sample with highest copolymer concentration, $\phi_{cop}=0.11$ contains most detailed information, it is used in the following to analyze the underlying microstructure. To this end the spectra are fitted by

$$I(Q)=\sum_N \frac{h_N}{(2\pi)^{1/2}s_N}\exp\left[-\frac{1}{2}\frac{(Q-Q_N)^2}{s_N^2}\right], \quad (8)$$

where Q_N is the position of the Nth order peak, s_N its width, and h_N its height. The dependence of the order of the maximum N on the value of the corresponding scattering vector Q_N is displayed in Fig. 7 for SAXS spectra taken at $T=333$ K. A linear least square fit passes through all data points and the origin (solid line): $Q_N=NQ_1$, showing that the first maximum corresponds to a first-order peak. The linear dependence of the magnitude of the scattering vector on the number of the peak indicates that the L_α phase has a lamellar structure.

To support this inference we calculated the repeat distance from sample composition and compared this value with those obtained from scattering spectra. Assuming single phase lamellae and a thickness of $\delta_s=(1\pm0.1)$ nm for the surfactant layer, both the repeat distance and the thickness of the alternating AOT-water-AOT-oil layers can directly be calculated from sample composition: for the value of the repeat distance one obtains

$$D_r^{comp}=\frac{2\delta_s}{\phi_s}\approx(33\pm3)\text{ nm} \quad (9)$$

and, for the thickness of the water and oil layers $D_{H_2O}=(6.3\pm0.6)$ nm, and $D_{oil}=(25.5\pm2)$ nm, respectively. As PEO is soluble in isooctane above ≈325 K we estimated the thickness of the oil layer using the volume fraction of copolymer and isooctane. On the other hand the position of the peaks are determined by the repeat distance [37],

$$Q_1^{SAXS}=\frac{2\pi}{D_r^{SAXS}}\approx0.18\text{ nm}^{-1}\Longrightarrow D_r\approx35\text{ nm}. \quad (10)$$

Hence D_r^{comp} and D_r^{SAXS} coincide within the error margin.

After having investigated the microstructure of the L_α phase we examine the influence of copolymer concentration on the scattering spectra. Figure 8 shows the scattering spectra for six different copolymer concentrations at 333 K. At this temperature all samples are in the L_α phase. Addition of the copolymer mainly leads to an increase of the number of peaks visible in the scattering spectra. For low copolymer concentration ($\phi_{cop}=0.012$) only a single peak is visible, whereas four peaks can be observed at $\phi_{cop}=0.11$. Peak positions shift slightly towards lower Q values, as the volume fraction of surfactant decreases slightly after the addition of the copolymer. (Of course the volume fractions of water and oil change, too. Note, however, that the repeat distance D_r only depends on ϕ_s.) The same observation also holds for other temperatures, because the scattering spectra depend only slightly on temperature as long as the microstructure of the samples remains lamellar. As the number of peaks is related to the ordering in the system [17], the latter increases significantly due to addition of copolymers.

Because PEO is solvable in isooctane at high temperatures it is not clear from the above measurements in how far the PEO end groups influence the stabilization and ordering of the lamellae. On the one hand the observed ordering may be due to connecting the lamellae by the copolymers, or on the other hand due to damping of oscillations by steric hinderance caused by copolymers mainly dissolved in the isooctane layers. In the latter case water layers are electrostatically stabilized. Figure 9 shows a SAXS spectrum of a PI homopolymer, dissolved

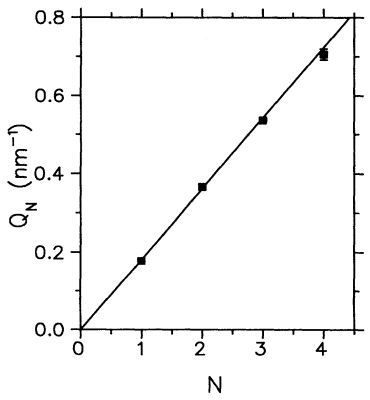

FIG. 7. Fitted value of the Nth small angle x-ray scattering maximum Q_N, $N\leq4$, versus order of the peak for a copolymer containing a water-oil-surfactant mixture at $T=333$ K with $\phi_{cop}=0.11$, or $R=20$ and $\phi_d=0.27$, $w_0=61.8$ [cf. Fig. 3(bottom)]. The solid line is the best linear fit going through the origin and all data points.

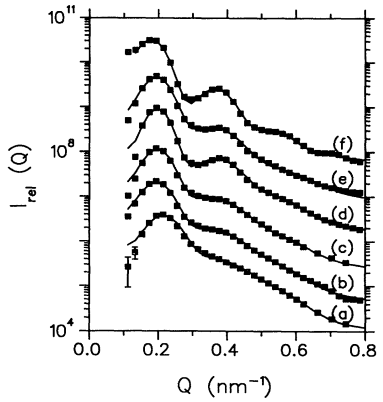

FIG. 8. Scattering intensity versus scattering vector for lamellar structure of water-AOT-isooctane-AOT layers containing different amounts of copolymer ($0.012\leq\phi_{cop}\leq0.11$). All scattering spectra are taken at 333 K. The solid lines yield least square fits to the data points by equidistant Gauss functions. Note that the number of peaks increases with polymer concentration. Copolymer concentration increases from bottom to top: (a) $\phi_{cop}=0.012$; (b) $\phi_{cop}=0.029$; (c) $\phi_{cop}=0.042$; (d) $\phi_{cop}=0.069$; (e) $\phi_{cop}=0.087$; (f) $\phi_{cop}=0.111$.

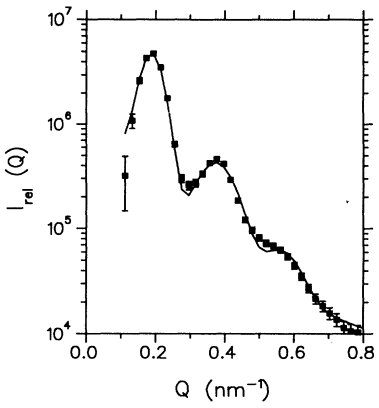

FIG. 9. Scattering intensity versus scattering vector for lamellar structure of water-AOT-isooctane-AOT layers containing a PI homopolymer, $\phi^{PI}_{homo}=0.09$, $w_0=61.8$, $\phi_d=0.27$. The scattering spectrum is taken at 333 K. The solid line yields a least square fit to the data points by equidistant Gauss functions.

in a water-AOT-isooctane mixture of equal composition as used before at $T=333$ K and polymer concentration of $\phi^{PI}_{homo}=0.09$. This optical birefringent sample remains single phase on an experimental time scale. Again several equidistant peaks can be observed. The spectrum is similar to those obtained from copolymer stabilized lamellae with $\phi_{cop}=0.087$, indicating that the stabilization and ordering is due to the PI coils dissolved in the isooctane layers. Hence, the addition of a lipophilic polymer to a water-oil-surfactant mixture induces stabilization of lamellae.

IV. DISCUSSION AND CONCLUSIONS

For the low-temperature droplet phase as well as for the high-temperature lamellar phase, we have shown that the addition of the copolymer leads to developing of order, leading to an increase in the number of peaks in SAXS-intensity spectra. In the droplet phase local ordering of droplets becomes important, and in the lamellar phase intralayer correlations increase significantly. In both situations the ordering of microphases grows under addition of copolymer. We expect that geometrical constraints form the origin. We will first discuss this for the droplet phase. In the droplet phase the hydrophilic copolymer end groups (PEO) are located in the water cores and isooctane forms a good solvent for the hydrophobic PI middle part. Thus, for high copolymer concentration the droplets are surrounded by a coat of PI, leading to constraints on the center-to-center approach distance of the water cores. This picture is similar to models explaining SAXS scattering profiles of miocrophase separated diblock copolymer systems into spherical domains. Similar to the droplets in a copolymer mediated microemulsion, these microdomains can be viewed as hard-core particles surrounded by a polymer layer. In the latter case the main contributions to the interaction free energy of two particles approaching each other are expected to result from the following (cf. [44]).

(i) A repulsive term due to the loss of configurational entropy of the polymer.

(ii) A repulsive term due to excluded volume interaction.

(iii) An attractive term due to van der Waals attraction between particles.

For high surface coverage and high molecular weight of the adsorbed chains it has been shown that the repulsive forces are dominant, causing a steeply increasing interaction energy with decreasing separation distance. For the copolymer coated droplet system investigated in the present paper we expect these forces to also play a role. However, the following additional effects due to the droplet structures should be considered.

(iv) For ionic microemulsions it has been shown that the attraction between droplets increases strongly with temperature [41,47].

(v) Addition of triblock copolymers to a microemulsion droplet phase leads to viscoelastic network formation [28]. This is caused by copolymers having their end groups in different droplets. In such a situation spatial displacement of the droplets directly influences the number of possible configurations of the PI coil. Therefore copolymers may give rise to an attractive interaction between droplets when the latter separate too far. Of course, not all copolymers connect droplets, but there is an equilibrium between copolymers having both end groups in the same and in different droplets.

By these considerations the influence of copolymers may be viewed as (in general nonlinear) springs between the droplets. Dependent on the molecular weight of the PI chain and on the value for the droplet-droplet distance the PI coil yields an extra attractive or repulsive contribution to the free energy of interaction. In our situation the average spacing between the droplets is smaller than the preferred end-to-end distance of the copolymer middle part. This results in strongly increased repulsive interactions between the droplets, leading to close packed structures of the copolymer coated droplets.

The high-temperature lamellar phase is built up by repeating water-surfactant-oil-surfactant layers. To obtain single phase lamellae, the water and the oil layers need to be stabilized. Two different stabilization forces will be considered in the following.

(a) Water layers: for the stabilization of the water layers repulsive electrostatic interactions due to partial ionization of the surfactant head groups need to be considered [18].

(b) Oil layers: The scattering spectra obtained from PI homopolymers and from copolymers dissolved in water-surfactant-isooctane mixtures are similar, showing that the PEO end groups do not influence the lamellar phase significantly. As PEO becomes increasingly lipophilic under increasing temperature, both, the copolymer and the PI homopolymer can be regarded as coils purely dissolved in isooctane. Movement of the lamellae directly influences the number of possible configurations of the coils. This gives rise to a repulsive interaction between

the surfactant monolayers enclosing the oil layers. This repulsive force increases with the number of springs per unit volume, i.e., with the polymer concentration.

To stabilize the oil layers, the polymer induced repulsive forces between the surfactant monolayers have to overwhelm the van der Wals attraction. In addition, increasing repulsive interactions hinder thermal fluctuations of single AOT monolayers and of the water swollen AOT bilayers (AOT-water-AOT). We expect that this leads to an increase of the effective bending rigidity of the water swollen AOT bilayers. Hence, it increases the correlation length of membranes, resulting in an enhancement of long range order [17].

By microcalorimetric measurements the present authors have shown that for ionic surfactant systems the transition of the microemulsion into a lamellar phase is entropy driven. As the lamellar phase is formed at higher temperatures than the microemulsion phase this is what one expects from the monotonicity of the entropy. On the other hand, this appears to be in contrast to some claims in the literature. E.g., Lee and Chen [48] refer to de Gennes and Taupin [8] to claim that "at moderate temperature and at high surfactant concentration a lamellar phase is bounded by an entropically more favorable isotropic microemulsion phase." Indeed, de Gennes and Taupin argued that for low values of the bending constant the surfactant monolayer can become extremely wrinkled, leading to a gain in entropy that is larger than the loss of free energy due to the departure from a periodic array. This apparent contradiction to the present findings might be due to electrostatic interactions or due to a nontrivial temperature dependence of the spontaneous radius of curvature and of the bending moduli.

The main conclusions of this paper are as follows: the solution of triblock copolymers with a hydrophilic-hydrophobic-hydrophilic structure in water-oil-surfactant systems preserves characteristic droplet and lamellar structures of the system. In the low-temperature droplet phase some polymers connect droplets, while in the lamellar phase the (co)polymers can be regarded as coils, purely dissolved in the oil layers. Its influence may be modeled by effective springs, that significantly enhance the ordering of the system. In addition they slow down the kinetics of the phase transition between the droplet and the lamellar structure, and significantly hinder phase separation of the system. This is fortunate for studying the phase transition and the lamellar phase. In the limit of low concentration, the addition of copolymers allows us to control typical time scales of phase separation of the high-temperature lamellar phase so that contributions to the latent heat to the structural transition from a droplet to a lamellar phase, and due to phase separation of the lamellar phase, can be separated. Taking advantage of this possibility we showed that the structural transition is entropy driven. For high copolymer concentration we observe ordered single phase droplet and lamellar structures. The latter show interlamellar spacings, which can hardly be stabilized by other means. Using homopolymers we show that this mechanism for stabilization is due to repulsive forces induced by the (co)polymer coils dissolved in the oil layers. In particular, the suppression of phase separation in lamellar structures is important for future experiments on properties of membranes as knowledge on the composition of the lamellar phase gives important clues for the interpretation of experimental data.

ACKNOWLEDGMENTS

One of the authors (D.V.) would like to thank F. Nallet and H. N. W. Lekkerkerker for stimulating discussions. The authors would like to thank Professor Seelig, Department of Biophysical Chemistry at the Biozentrum, Basel, for hospitality during microcalorimetric measurements and P. Ganz for his service during these measurements. This work was supported in part by the Swiss National Science Foundation.

[1] H. N. W. Lekkerkerker, Physica A **176**, 1 (1991).
[2] P. N. Pusey, W. van Megan, S. M. Underwood, P. Barlett, and R. H. Ottewill, Physica A **176**, 16 (1991).
[3] B. J. A. Ackerson, Physica A **174**, 15 (1991).
[4] F. S. Bates, R. E. Cohne, and C. V. Berney, Macromolecules **15**, 589 (1982); F. S. Bates, Annu. Rev. Phys. Chem. **41**, 525 (1990).
[5] R. W. Richards and J. L. Thomason, Macromolecules **16**, 982 (1983).
[6] J. Yang, G. Wegner, and R. Koningsveld, Colloid Polym. Sci. **270**, 1080 (1992).
[7] L. Golubovic and T. C. Lubensky, Phys. Rev. A. **41**, 4343 (1990).
[8] P. G. de Gennes and C. Taupin, J. Phys. Chem. **86**, 2294 (1982).
[9] G. Gompper and M. Schick, Phys. Rev. B **41**, 9148 (1990).
[10] M. Kotlarchyk, E. Y. Sheu, and M. Capel, Phys. Rev. A **46**, 928 (1992).
[11] R. Strey, Ber. Bunsenges, Phys, Chem. **97**, 742 (1994).
[12] M. Kotlarchyk, S.-H. Chen, J. S. Huang, and M. W. Kim, Phys. Rev. Lett. **53**, 941 (1984).
[13] W. Jahn and R. Strey, J. Phys. Chem. **92**, 2294 (1988).
[14] D. Roux and C. R. Safinya, J. Phys. (Paris) **49**, 307 (1988).
[15] F. Nallet, D. Roux, and J. Prost, Phys. Rev. Lett. **62**, 276 (1989); J. Phys. (Paris) **50**, 3147 (1989).
[16] R. Strey, R. Schomäcker, D. Roux, F. Nallet, and U. Olsson, J. Chem. Soc. Faraday Trans. **86**, 2253 (1990).
[17] C. R. Safinya, E. B. Sirota, D. Roux, and G. S. Smith, Phys. Rev. Lett. **62**, 1134 (1989).
[18] P. Pincus, J.-F. Joanny, and D. Andelman, Europhys. Lett. **11**, 763 (1990).
[19] W. Helfrich, J. Phys. (Paris) **46**, 1263 (1985).
[20] D. Roux, F. Nallet, E. Freyssingeas, G. Porte, P. Bassereau, M. Skouri, and J. Marignam, Europhys. Lett. **17**, 575 (1992).
[21] R. Schomäcker and R. Strey, J. Phys. Chem. **98**, 3908

(1994).
[22] H.-F. Eicke, U. Hofmeier, Ch. Quellet, and U. Zölzer, Prog. Colloid Polym. Sci. **90**, 165 (1992).
[23] Ch. Quellet, H.-F. Eicke, G. Xu, and Y. Hauger, Macromolecules **23**, 3347 (1990); R. Hilfiker,, H.-F. Eicke, Ch. Steeb, and U. Hofmeier, J. Phys. Chem. **95**, 1478 (1991).
[24] R. Hilfiker, Ber. Bunsenges. Phys. Chem. **95**, 1227 (1991).
[25] F. Stieber, U. Hofmeier, H.-F. Eicke, and G. Fleischer, Ber. Bunsenges. Phys. Chem. **97**, 812 (1993).
[26] J. W. Gibbs, *Collected Works* (Dover, New York, 1961), Vol. 1; J. D. Van der Waals and Ph. Kohnstamm, *Lehrbuch der Thermodynamik* (Barth, Leipzig, 1912), Vol. 2; F. A. H. Schreinemakers, in *Die Heterogenen Gleichgewichte vom Standpunkt der Phasenlehre,* edited by H. W. Bakhuis Rozeboom (Vieweg, Braunschweig, 1913), Vol. 3.
[27] D. Vollmer, U. Hofmeier, and H.-F. Eicke, J. Phys. II (France) **2**, 1677 (1992).
[28] U. Zölzer, H.-F. Eicke, J. Phys. II (France) **2**, 2207 (1992).
[29] M. A. van Dijk, J. G. H. Joosten, Y. K. Levine, and D. Bedeaux, J. Phys. Chem. **93**, 2506 (1989).
[30] *Polymer Handbook,* 2nd ed. (Wiley, New York, 1974).
[31] J.-F. Bodet, J. R. Bellare, H. T. Davis, L. E. Scriven, and W. G. Miller, J. Phys. Chem. **92**, 1898 (1988).
[32] M. Müller, N. Meister, and H. Moor, Microscopie (Wien) **36**, 129 (1980).
[33] T. Boublik, V. Fried, and E. Hála, *The Vapor Pressure of Pure Substances* (Elsevier, New York, 1973), p. 415.
[34] G. R. Strobel, Acta Crystallogr. A **26**, 367 (1970).
[35] D. Vollmer and P. Ganz, J. Chem. Phys (to be published).
[36] The copolymer induced shift of the percolation temperature is investigated in H.-F. Eicke, M. Gauthier, and H. Hammerich, J. Phys. II (France) **3**, 255 (1993).
[37] For the analysis of the scattering vectors Q_N one has to consider that besides the repeat distance D_r, the lamellae are characterized by two further length scales D_{H_2O} and D_{oil}, giving the thickness of the water and oil layers, respectively. The influence of the water and oil layers on the scattering intensity via the structure function S_k can be estimated by treating the lamellae as a periodic system with a two point basis $d_1=(0,0,-\frac{1}{2}D_{H_2O})$ and $d_2=(0,0,\frac{1}{2}D_{H_2O})$. Therefore

$$S_k=\sum_{j=1}^{2} e^{i\mathbf{K}\cdot\mathbf{d}_j}=2\cos\left[\frac{2\pi n D_{H_2O}}{D_r}\right], \tag{11}$$

where $\mathbf{K}=(2\pi/D_r)\hat{\mathbf{z}}$ is a reciprocal lattice vector. This shows that the internal structure of the repeat units leads to a modulation of scattering intensities, but does not influence the position of the peaks. The latter are only determined by the repeat distance. Note that one obtains the same result, when choosing D_{oil} for the second length scale, as $D_{oil}=D_r-D_{H_2O}$.
[38] J. T. Brooks, C. M. Marques, and M. E. Cates, Europhys. Lett. **14**, 713 (1991); J. T. Brooks and M. E. Cates, J. Chem. Phys. **99**, 5467 (1993).
[39] R. Hilfiker, H.-F. Eicke, W. Sager, C. Steeb, U. Hofmeier, and R. Gehrke, Ber. Bunsenges. Phys. Chem. **94**, 677 (1990).
[40] C. Robertus, J. G. H. Joosten, and Y. K. Levine, Phys. Rev. A **42**, 4820 (1990).
[41] F. Zernike and J. A. Prins, Z. Phys. **41**, 184 (1927).
[42] L. S. Ornstein and F. Zernike, Proc. Acad. Sci. Amsterdam **17**, 793 (1914).
[43] J. K. Percus and G. J. Yevick, Phys. Rev. **110**, 1 (1958).
[44] D. J. Kinning and E. L. Thomas, Macromolecules **17**, 1712 (1984).
[45] P. G. Fournet, Acta Crystallogr. **4**, 293 (1951).
[46] N. W. Ashcroft and N. D. Mermin, *Solid State Physics* (Holt-Saunders, Philadelphia, 1976).
[47] D. Vollmer, J. Vollmer, and H.-F. Eicke, Europhys. Lett. **26**, 389 (1994).
[48] D. D. Lee and S. H. Chen, Phys. Rev. Lett. **73**, 106 (1994).

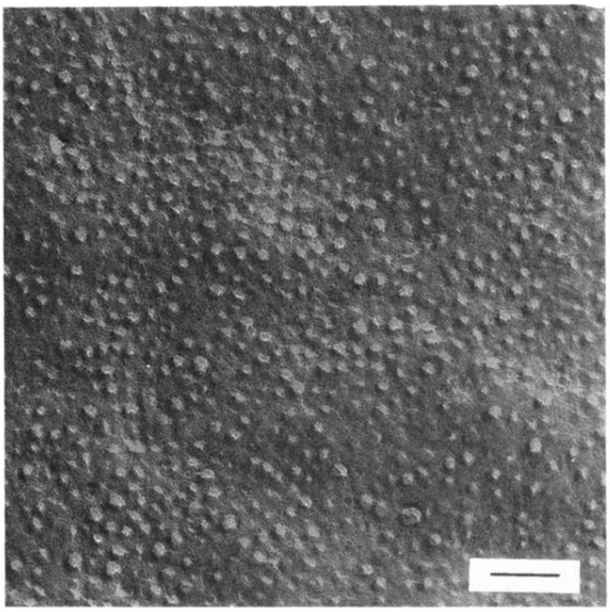

FIG. 2. Freeze-fracture electron micrograph of a copolymer mediated water-in-oil microemulsion at 294±0.5 K in the one-phase region. Water droplets are embedded in an oil matrix. The composition of the copolymer mediated microemulsion is given by: $R=8$, $w_0=61.8$, $\phi_d=0.27$. The length of the bar corresponds to 200 nm.